

Machine Learning-Guided Design of Perovskite Oxides for High-Temperature Oxygen Sensing

**Manh Tien Nguyen¹, Leebyn Chong^{1,2}, Yueh-Lin Lee^{1,2}, Dan Sorescu¹,
Yuhua Duan¹**

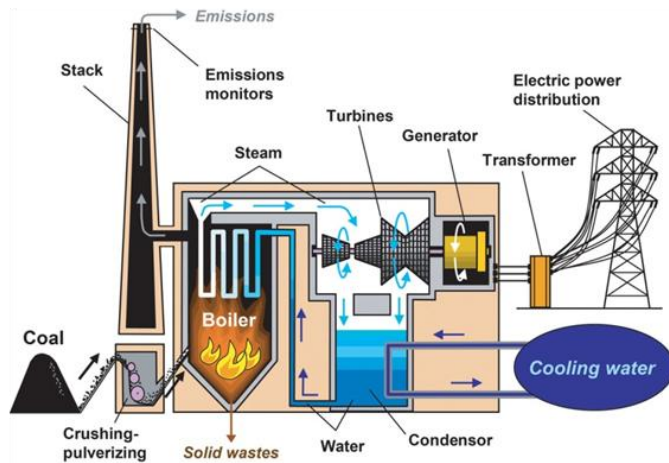
¹ National Energy Technology Laboratory, U. S. Department of Energy, Pittsburgh, PA, USA

² NETL Support Contractor, 626 Cochran Mill Road, Pittsburgh, PA, USA

Introduction

- Real-time gas monitoring in harsh combustion environments requires robust high-temperature sensors
- Perovskite oxides (ABO_3) offer superior thermal stability and tunable properties through A/B-site doping
- Machine learning combined with first-principles calculations accelerates materials discovery

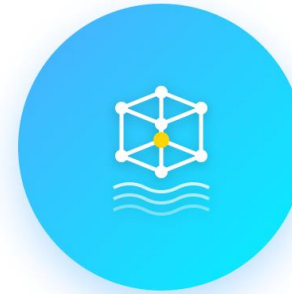
Fossil-/Nuclear-based power plants



Harsh Environment

High-temperature combustion conditions require robust materials

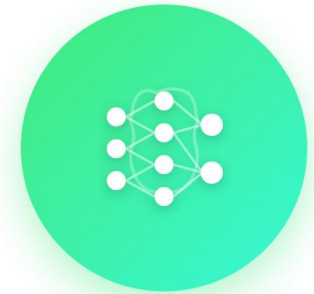
300-1000°C



Material Stability + High Sensitivity

Perovskite oxides with tunable properties and thermal resilience

ABO_3 Structure



ML Discovery

Machine learning screens millions of candidates to accelerate materials design

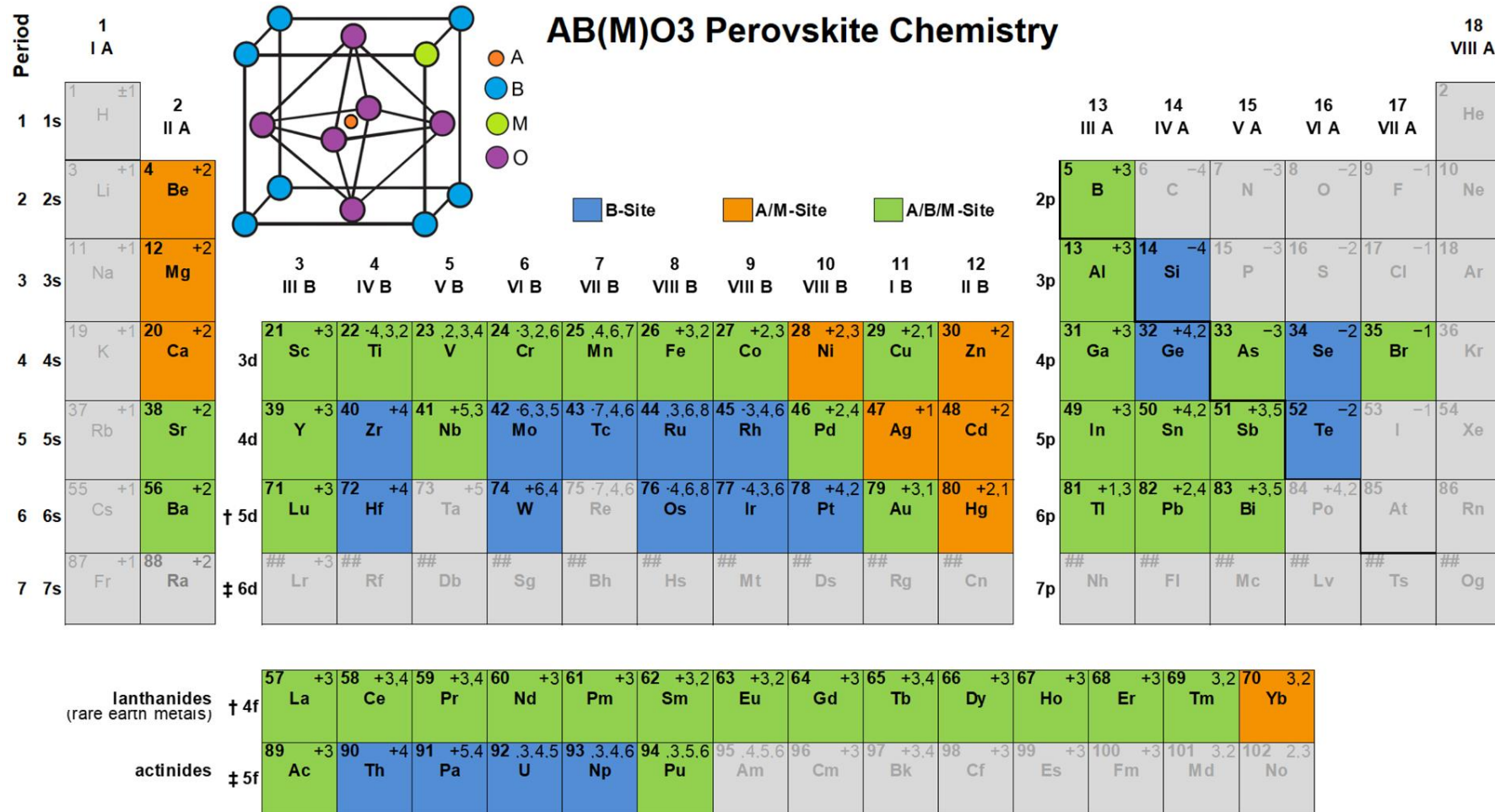
187M → Top Candidates

ML-driven Discovery Pipeline



- Generated 187 million ABO₃ combinations from 13 A-site (Sr, La, Ca, Ba...) and 36 B-site (Ti, Nb, Dy...) elements with varied ratios

Initial Composition Generation



187 million compositions



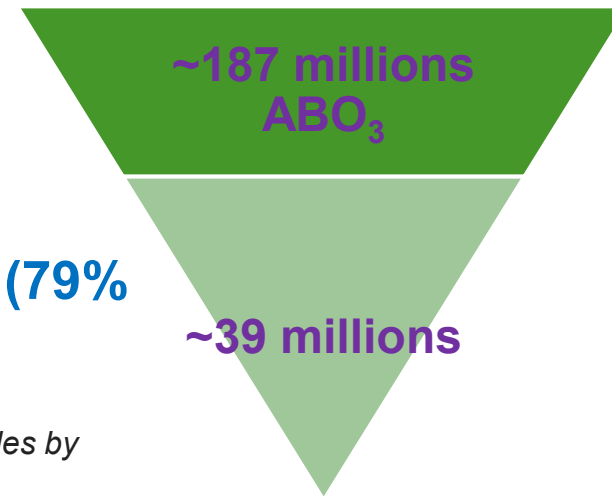
A site	Ba	Bi	Ca	Ce	Gd	La	Mg
	Nd	Pr	Sm	Sr	Y	Yb	
B site	Al	Be	Ca	Ce	Co	Cr	
	In	La	Lu	Mg	Mn	Mo	
	Sn	Tb	Th	Ti	V	W	
	Cu	Dy	Er	Fe	Ga	Gd	
	Nb	Nd	Ni	Pr	Sc	Si	
	Y	Yb	Zn	Zr	Hf	Sm	

Priya, Pikee, and Narayana R. Aluru. "Accelerated design and discovery of perovskites with high conductivity for energy applications through machine learning." *npj Computational Materials* 7, no. 1 (2021): 90.

Stability Prediction

Database	Features	Target
1120 ABO ₃ from the ICSD database by Zhai et al. and literature by Priya et al.	Site-specific elemental features, including cation-oxygen bond distance, Mendeleev number, oxidation states, and ionic radius	946 Perovskite/ 174 not Perovskite

- A gradient boosting classification model predicted perovskite stability
- Mean F1 score of 0.95 ± 0.02 on 5-fold cross-validation
- Reduced candidates from ~187M to ~39M stable compositions (79% reduction)

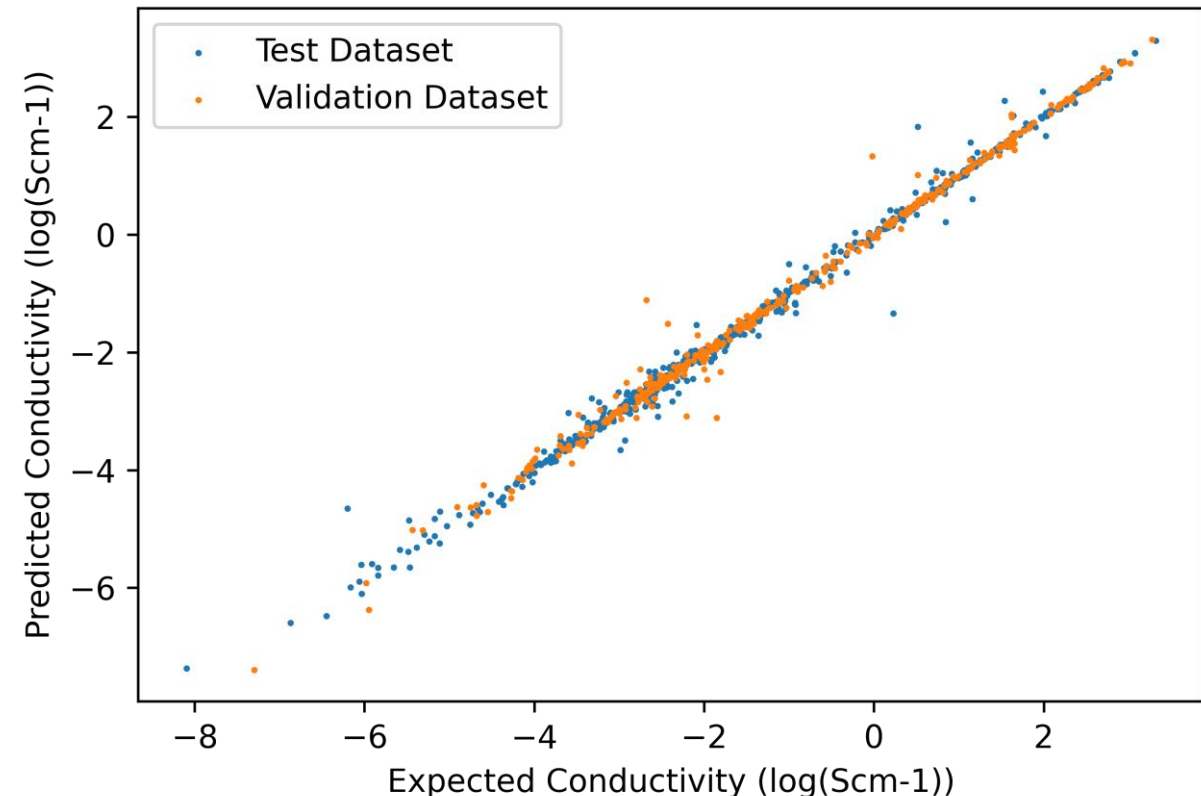


Zhai, X., Ding, F., Zhao, Z., Santomauro, A., Luo, F. and Tong, J., 2022. Predicting the formation of fractionally doped perovskite oxides by a function-confined machine learning method. *Communications Materials*, 3(1), p.42.

Conductivity Prediction

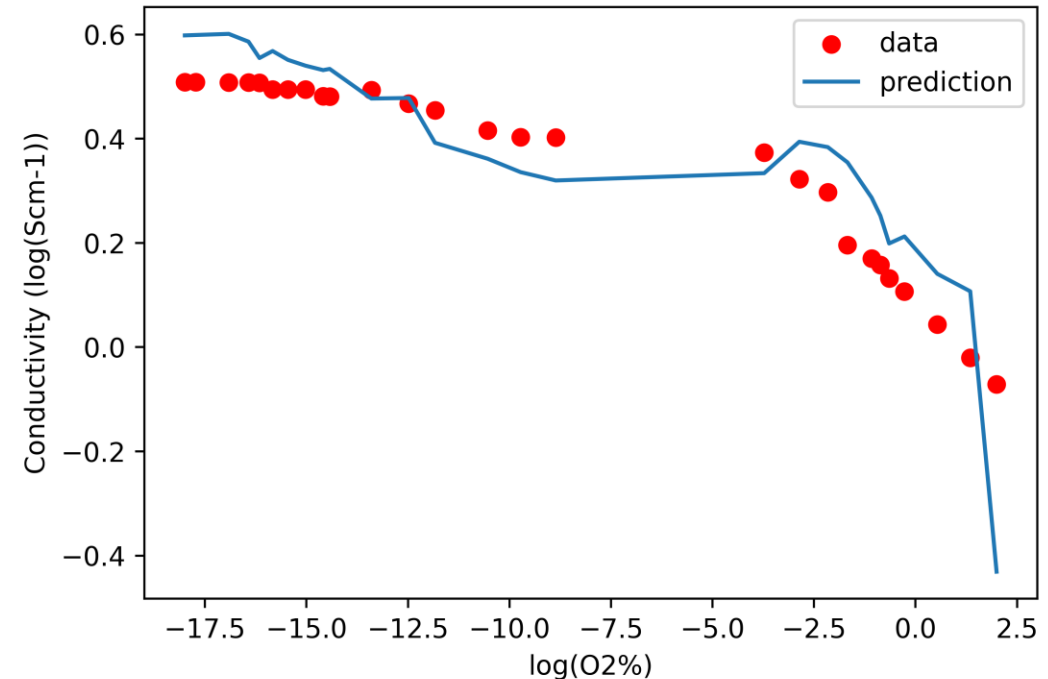
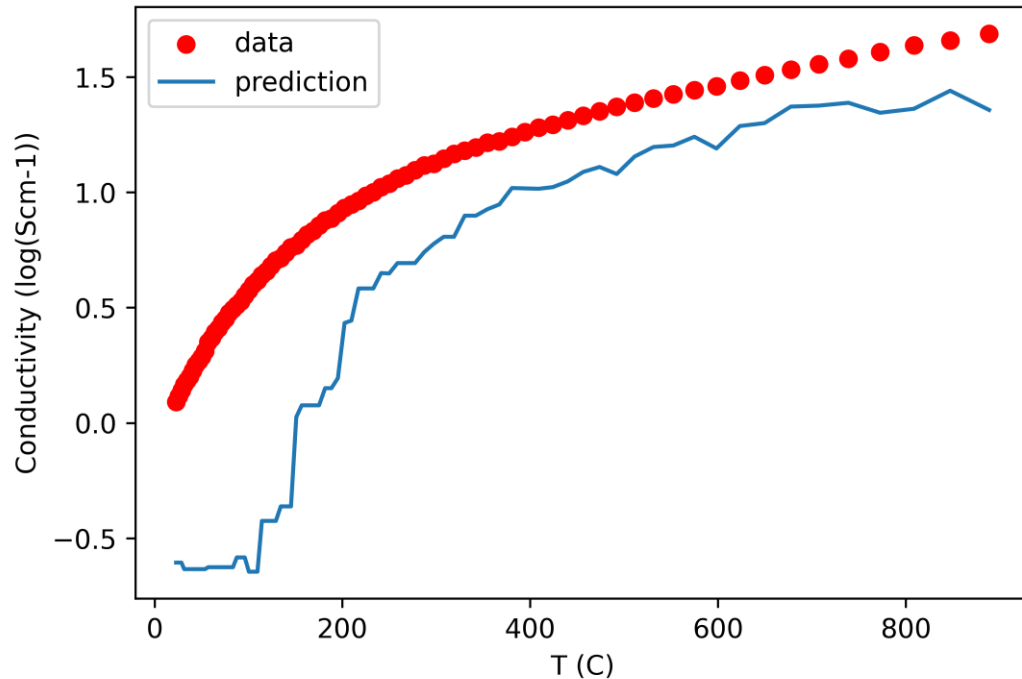
- XGBoost regression model: 600 estimators, max depth 10, trained on the dataset reported by Priya et al.
- 100 features derived from Materials Project database (oxide properties) and Shannon tables (elemental properties)
- Top predictors: ionic radius, electronegativity, atomic mass, oxide formation energy
- Performance: $R^2 = 0.99$, RMSE = 0.18

Priya, Pikee, and Narayana R. Aluru. "Accelerated design and discovery of perovskites with high conductivity for energy applications through machine learning." *npj Computational Materials* 7, no. 1 (2021): 90.



Conductivity Prediction

- Predicted conductivity trends match experimental ground truth for a given perovskite across temperature and oxygen partial pressure
- Validated model fitness enables oxygen sensitivity quantification



Top Oxygen Sensing Candidates

- 39M candidates screened with full Temperature-pO₂ conductivity profiles
- Materials ranked by oxygen-conductivity gradient (sensitivity metric)
- Top candidates show 3-order-magnitude conductivity change across pO₂ range
- Literature validation confirms model predictions

#	Composition	pO ₂ (%)	Temp (°C)	Δlog ₁₀ (Conductivity)	Experimental reported
1	La _{0.4} Sr _{0.4} TiO ₃	1e-18 - 100	930	3.0789201	La _{0.4} Sr _{0.4} TiO ₃
2	La _{0.6} Sr _{0.1} TiO ₃	1e-18 - 100	930	2.9785082	
3	La _{0.45} Sr _{0.25} TiO ₃	1e-18 - 100	930	2.924773	
4	La _{0.55} Sr _{0.15} TiO ₃	1e-18 - 100	930	2.9047394	
5	La _{0.5} Sr _{0.2} TiO ₃	1e-18 - 100	930	2.887693	
6	La _{0.3} Sr _{0.5} TiO ₃	1e-18 - 100	930	2.7824388	
7	Ba _{0.25} Y _{0.45} TiO ₃	1e-18 - 100	930	2.7820268	
8	La _{0.4} Sr _{0.3} Nb _{0.05} Ti _{0.95} O ₃	1e-18 - 100	930	2.7802086	
9	Ba _{0.25} Y _{0.45} Nb _{0.05} Ti _{0.95} O ₃	1e-18 - 100	930	2.7801607	
10	La _{0.25} Sr _{0.55} Nb _{0.05} Ti _{0.95} O ₃	1e-18 - 100	930	2.7787879	

Interactive Web Tool

- An interactive web tool has been developed to enable researchers to leverage the predictive power of the ML model
- The web tool allows users to input perovskite compositions and obtain ranking of promising candidates with conductivity profiles, and O₂-conductivity gradients

Enter Conditions for Material Prediction

pO₂ ranges (2 values, comma-separated):

Temperature Values (°C) :
A-site Elements (select one or more, leave blank to include all):

Ba Bi Ca Ce Gd La Mg Nd Pr Sm Sr Y Yb

B-site Elements (select one or more, leave blank to include all):

Al Be Ca Ce Co Cr Cu Dy Er Fe Ga Gd Hf In La Lu Mg Mn

Mo Nb Nd Ni Pr Sc Si Sn Tb Th Ti V W Y Yb Zn Zr

A-site Element Count (1 or 2, empty means no filtering):

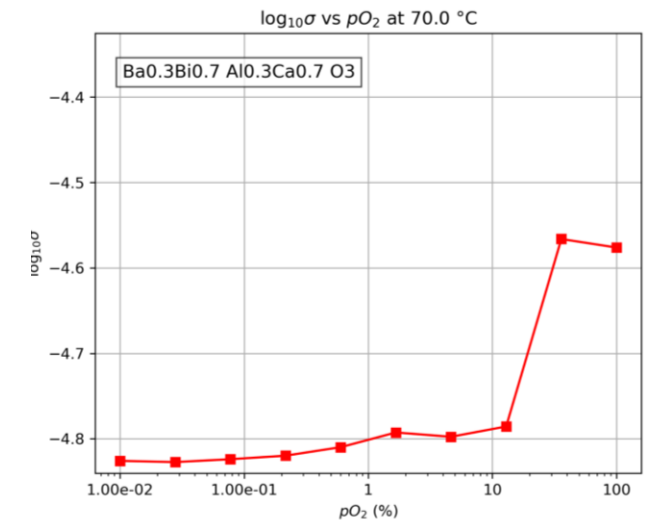
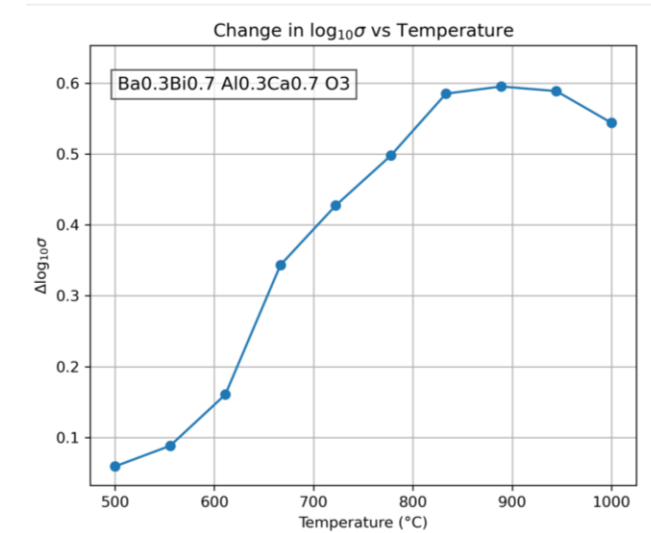
B-site Element Count (1 or 2, empty means no filtering):

Interactive Web Tool

Output of the web tool:

Top 10 Materials for Selected Conditions

Rank	ABO ₃ Composition	Temperature (°C)	pO ₂ Range (%)	Conductivity Change $\Delta\sigma$ (log ₁₀ (S/cm))
1	Ba _{0.3} Bi _{0.7} Al _{0.3} Ca _{0.7} O ₃	70.0	1e-02 - 100	0.24959039688110352
2	Ba _{0.3} Bi _{0.7} Be _{0.1} Ca _{0.9} O ₃	70.0	1e-02 - 100	0.24631690979003906
3	Ba _{0.3} Bi _{0.7} Al _{0.2} Ca _{0.8} O ₃	70.0	1e-02 - 100	0.2430119514465332
4	Ba _{0.3} Bi _{0.7} Al _{0.4} Ca _{0.6} O ₃	70.0	1e-02 - 100	0.23980045318603516
5	Ba _{0.3} Bi _{0.7} Al _{0.1} Ca _{0.9} O ₃	70.0	1e-02 - 100	0.23726129531860352
6	Ba _{0.3} Bi _{0.7} Be _{0.2} Ca _{0.8} O ₃	70.0	1e-02 - 100	0.2346029281616211
7	Ba _{0.3} Bi _{0.7} Be _{0.3} Ca _{0.7} O ₃	70.0	1e-02 - 100	0.21727752685546875
8	Ba _{0.3} Bi _{0.7} Ca O ₃	70.0	1e-02 - 100	0.1578836441040039
9	Ba _{0.6} Bi _{0.4} Be _{0.7} Ca _{0.3} O ₃	70.0	1e-02 - 100	0.1559600830078125
10	Ba _{0.4} Bi _{0.6} Be _{0.6} Ca _{0.4} O ₃	70.0	1e-02 - 100	0.1464672088623047



Density Functional Theory Analysis

➤ ML predictions at 700°C with 1-20% O₂ range guide DFT analysis

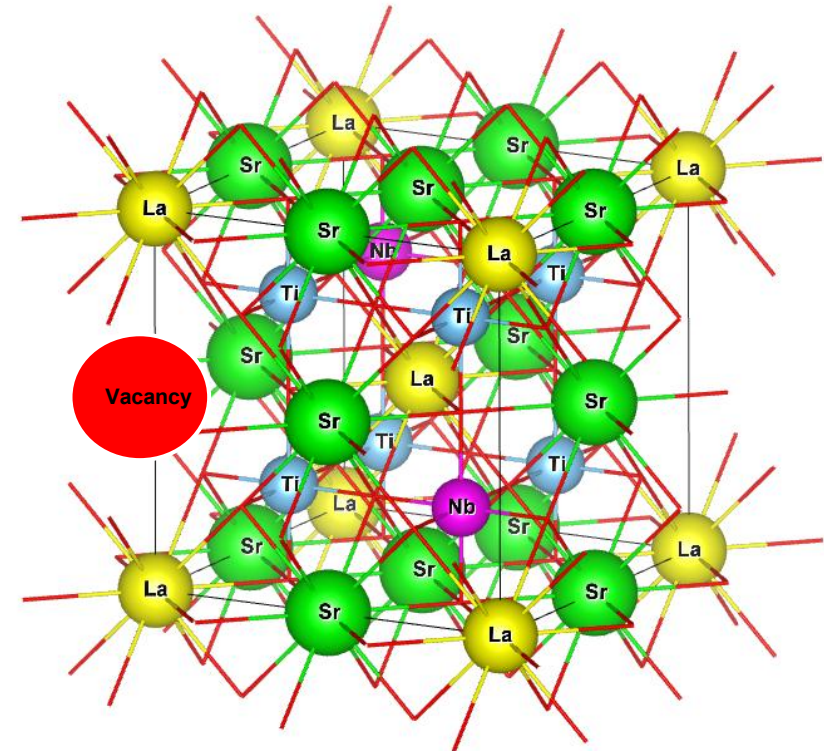
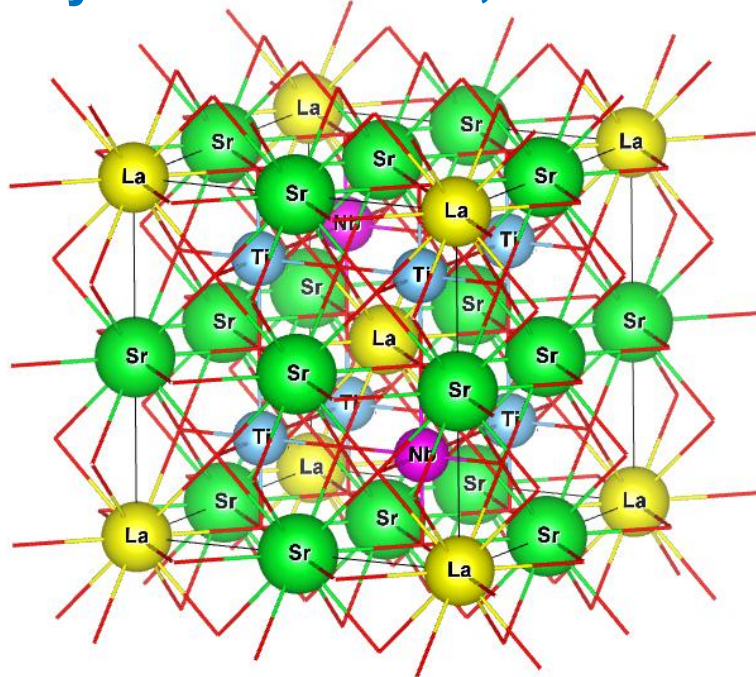
#	Conductivity change	PO2 Range (%)	Temperature (oC)	Material
1	0.8612474	1-20	700	La _{0.2} Sr _{0.6} Nb _{0.2} Ti _{0.8} O ₃
2	0.6170686	1-20	700	La _{0.2} Sr _{0.6} Nb _{0.15} Ti _{0.85} O ₃
3	0.615512	1-20	700	La _{0.4} Sr _{0.3} Nb _{0.15} Ti _{0.85} O ₃
4	0.6091372	1-20	700	La _{0.2} Sr _{0.6} Nb _{0.1} Ti _{0.9} O ₃
5	0.5975531	1-20	700	Nd _{0.2} Sr _{0.6} Nb _{0.15} Ti _{0.85} O ₃
6	0.5874653	1-20	700	Ba _{0.45} Ca _{0.45} Nb _{0.2} Ti _{0.8} O ₃
7	0.56509346	1-20	700	Gd _{0.2} Sr _{0.6} Nb _{0.1} Ti _{0.9} O ₃
8	0.5614067	1-20	700	Sm _{0.2} Sr _{0.6} Nb _{0.15} Ti _{0.85} O ₃
9	0.56001383	1-20	700	La _{0.2} Sr _{0.6} Nb _{0.05} Ti _{0.95} O ₃
10	0.53898513	1-20	700	Pr _{0.4} Sr _{0.3} Nb _{0.15} Ti _{0.85} O ₃

➤ La_{0.2}Sr_{0.6}Ti_yNb_(1-y)O₃ series (y = 0.8, 0.85, 0.9, 0.95) selected for validation

➤ Predicted that higher y values show decreased sensitivity (inverse correlation)

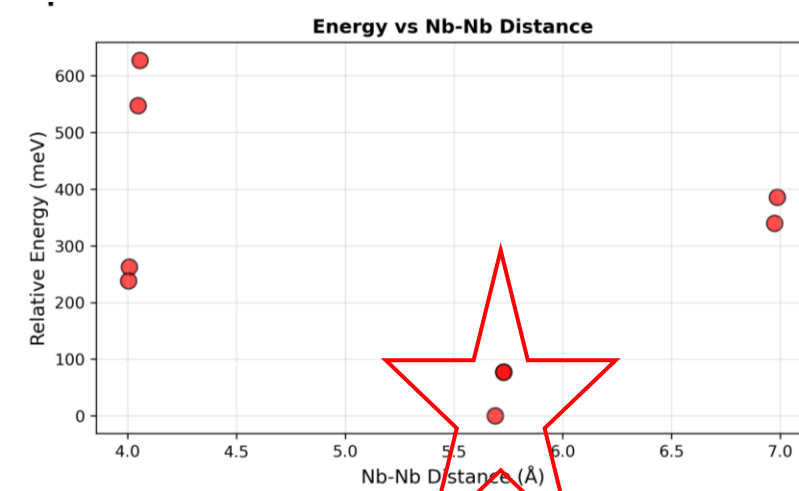
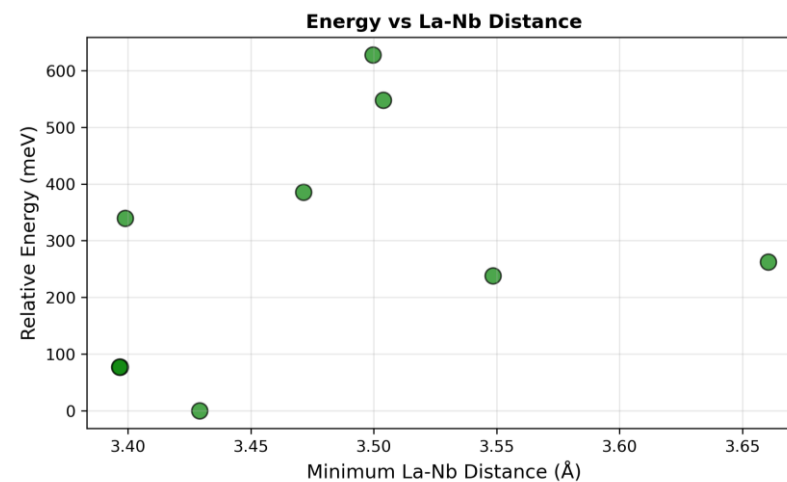
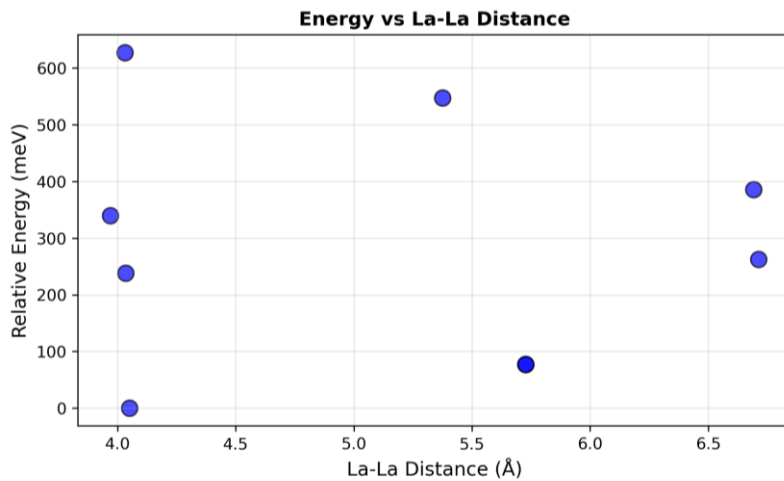
DFT Structural Analysis

- PAW-PBE+U functional in generalized gradient approximation
- $\text{La}_{0.2}\text{Sr}_{0.6}\text{Ti}_{0.8}\text{Nb}_{0.2}\text{O}_3$ supercell: 7.8 Å cubic lattice
- Dopant separations: La-La = 6.76 Å, Nb-Nb = 6.76 Å, La-Nb = 3.38 Å
- Sr vacancy proximity: Sr/La = 3.91 Å, Ti/Nb = 3.38 Å



Dopant Configuration Optimization

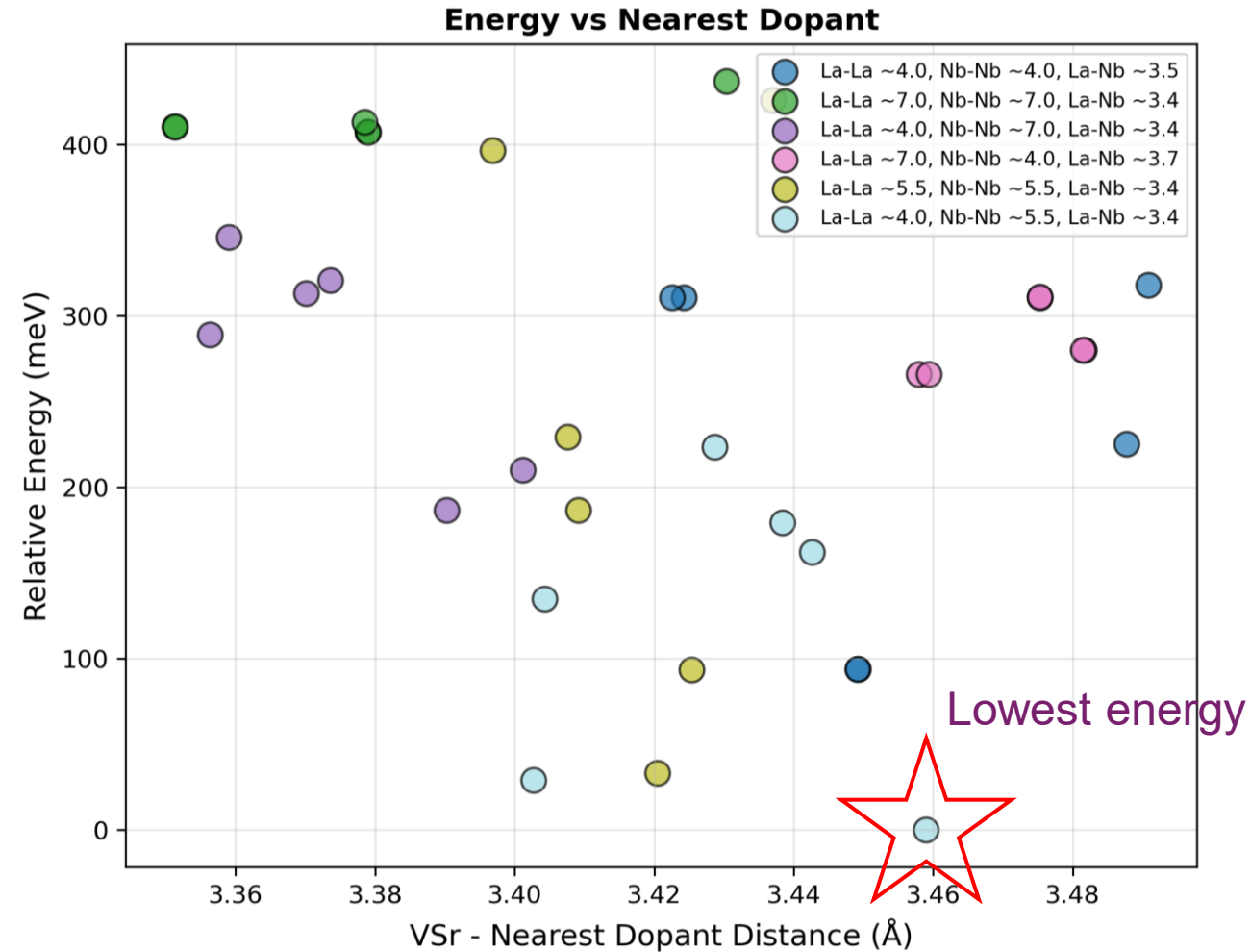
- 8 structural models tested for non-vacancy $\text{La}_{0.2}\text{Sr}_{0.8}\text{Ti}_{0.8}\text{Nb}_{0.2}\text{O}_3$
- Ground state energy vs. dopant distances (La-La, Nb-Nb, La-Nb)
- Lowest energy configuration identified



Lowest energy

Vacancy Configuration Optimization

- 42 structural models with Sr vacancy for $\text{La}_{0.2}\text{Sr}_{0.6}\text{Ti}_{0.8}\text{Nb}_{0.2}\text{O}_3$
- Energy landscape mapped across Sr vacancy-dopant separations
- Lowest-energy configuration selected for property calculations



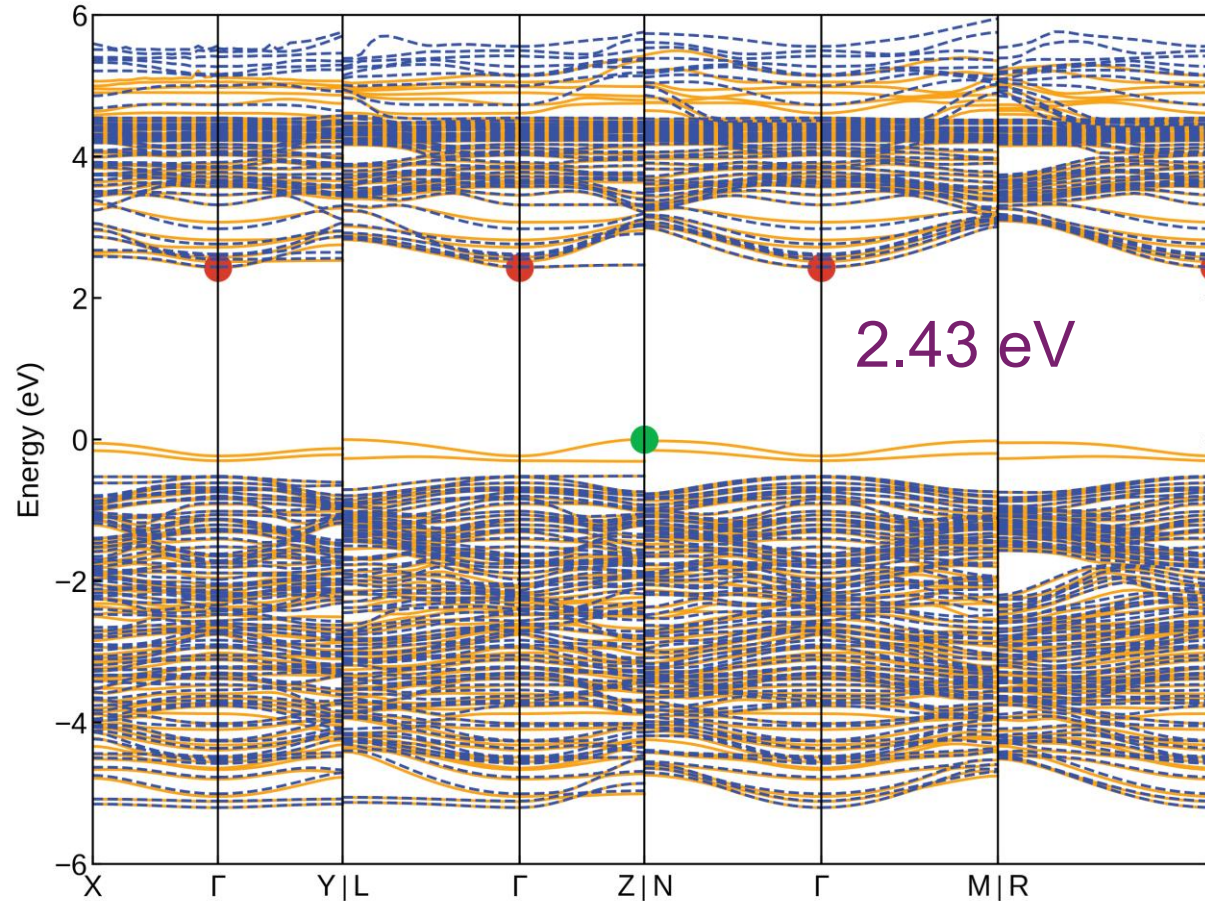
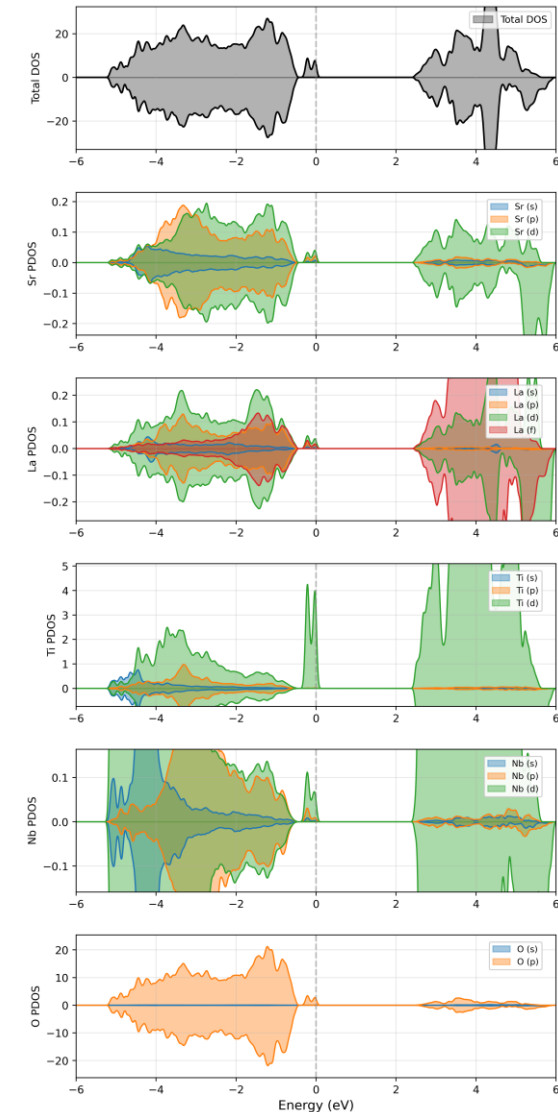
Formation Energy

- Formation energy of optimized $\text{Sr}_{0.6}\text{La}_{0.2}\text{Ti}_{0.8}\text{Nb}_{0.2}\text{O}_3$ structure
- Thermodynamic stability confirmed through DFT calculations

$$\Delta E_f = E_{\text{bulk}} - n_{\text{Sr}}E_{\text{Sr}} - n_{\text{Ti}}E_{\text{Ti}} - n_{\text{La}}E_{\text{La}} - n_{\text{Nb}}E_{\text{Nb}} - n_{\text{O}}\frac{1}{2}E_{\text{O}_2}$$

Formation energy (eV)	DFT	G(300K)	G(700k)
SrTiO_3	-16.82	-16.05	
$\text{Sr}_{0.6}\text{La}_{0.2}\text{Ti}_{0.8}\text{Nb}_{0.2}\text{O}_3$	-16.38	-15.54	-14.52

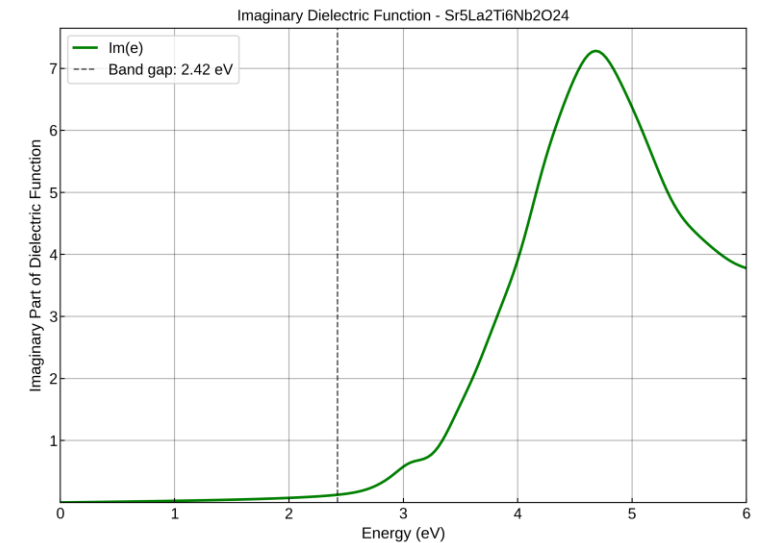
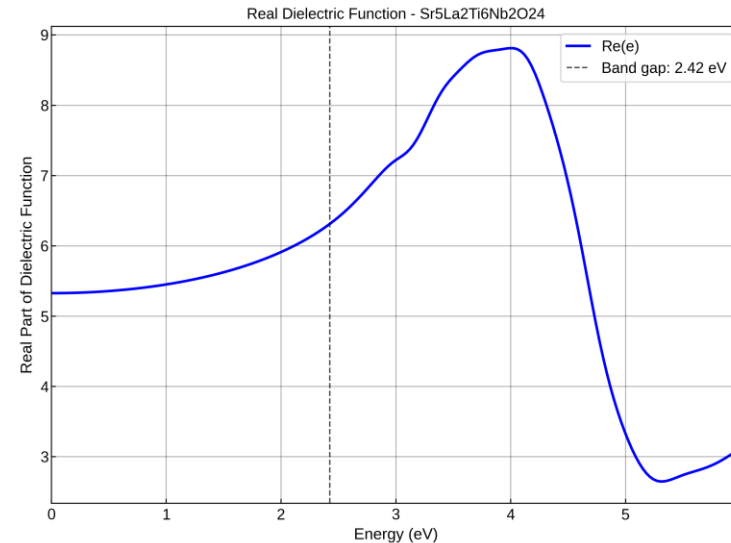
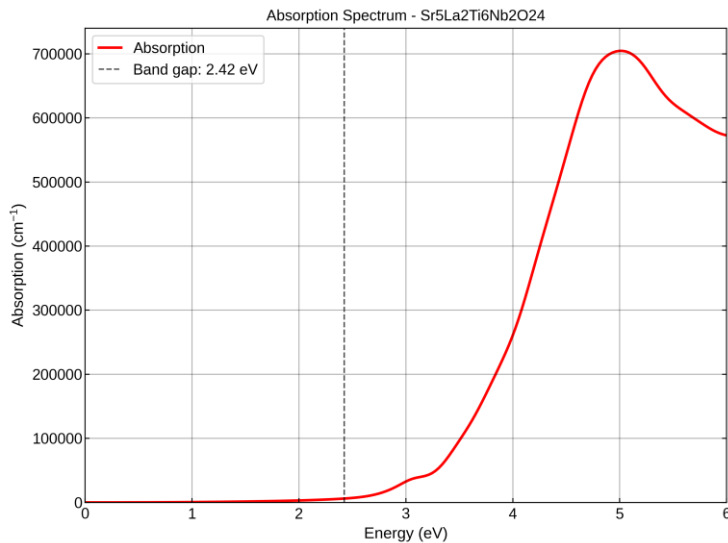
Electronic Structure



- Band structure reveals semiconductor behavior
- Density of states shows contributions from Sr, La, Ti, Nb, and oxygen orbitals

- Optical properties calculated from frequency-dependent dielectric function
 - Real/imaginary dielectric components characterize optical response

$$\varepsilon(\omega) = \varepsilon_1(\omega) + i\varepsilon_2(\omega) = (n + ik)^2 = \frac{4\pi i}{\omega} \sigma(\omega)$$



- Developed ML-DFT pipeline to screen 187M perovskite compositions for O₂ sensing
- Identified high-sensitivity candidates (3-order conductivity change)
- Validated Sr_{0.6} La_{0.2} Ti_{0.8} Nb_{0.2} O₃ as promising material through DFT
- Accelerated materials discovery for harsh-environment sensors for combustion monitoring, aerospace propulsion, industrial process control
- Future Work: Experimental synthesis and sensor device fabrication

Acknowledgement

We thank the computational resource at NETL

THANK YOU!

